



Corrosion and Dye

Elixir Corrosion & Dye 83 (2015) 32747-32754

Elixir
ISSN: 2229-712X

Senesio Extract as Green Corrosion Inhibitor for Copper in Nitric Acid Solutions

A.S.Fouda, H.M.Kila, A. Attia and A.M.Salem

Department of Chemistry, Faculty of Science, Mansoura and Zagazig Universities, Egypt.

ARTICLE INFO

Article history:

Received: 20 April 2015;

Received in revised form:
25 May 2015;

Accepted: 30 May 2015;

Keywords

Corrosion inhibition,
Plant extracts,
Copper, Nitric acid,
Green inhibitor.

ABSTRACT

The use of inhibitors for the control of corrosion of metals which are in contact with aggressive environment is an accepted practice. It is needless to point out the importance of cheap, safe inhibitors of corrosion. Plant extracts have become important as an environmentally acceptable, readily available and renewable source for wide range of inhibitors. The inhibition of the corrosion of copper in nitric acid solutions by senesio extract has been studied using chemical and electrochemical techniques. Inhibition was found to increase with increasing concentration of the senesio extract. Senesio extract is a rich source of ingredients which have very high inhibition efficiency. The adsorption of senesio extract on copper surface was found to obey Langmuir adsorption isotherm. The polarization data revealed that senesio extract acts as mixed type inhibitors. The surface morphology was analyzed.

© 2015 Elixir All rights reserved.

Introduction

Copper has been in use since ancient times and it has played an important role in the human life history due to its high corrosion resistance, its mechanical properties, ease of workability and good heat transfer properties. Copper is resistant toward the influence of atmosphere and many chemicals.

The possibility of the copper corrosion prevention has attracted many researchers so until now numerous possible extracts have been investigated. Amongst them there are inorganic extracts [1].

Copper metal surfaces can undergo oxidation when in contact with a gas, a liquid or a solid oxidizer. The process of metal loss due to oxidation is also called corrosion. Corrosion of base metal contacts, before and during the fabrication cycle can have negative consequences on performance, plating, appearance and in extreme cases result in component failure and costly reclaiming operations.

The use of copper corrosion extracts in such conditions is necessary since no protective passive layer can be expected. The possibility of the copper corrosion prevention in different aqueous solutions has attracted many researchers so until now numerous possible extracts have been investigated.

Some investigations have in recent time been made into the corrosion inhibiting properties of natural products of plant origin, which have been found to generally exhibit good inhibition efficiencies [2-12].

This area of research is of much importance because in addition to being inexpensive, readily available and renewable sources of materials, plant products are environmentally friendly and ecologically acceptable. Plant products are organic in nature and some of the constituents including tannins, organic and amino acids, alkaloids and pigments are known to exhibit inhibiting action.

The aim of this research is to study the corrosion inhibition of copper in 1 M HNO₃ solutions using senesio extract as corrosion extract using different techniques.

Experimental Method

Materials and solutions

The experimental measurements were carried out in 1M HNO₃ solution in absence and presence of various concentrations of senesio extract.

Methods used for corrosion measurements

Weight loss tests

For weight loss measurements, square specimens of size 2 x 2 x 0.2cm were used. The specimens were first abraded to a mirror finish using different grades (320–1200 grade) of emery papers, degreased with acetone, washed with bidistilled water and dried with soft paper before weighed and immersed in to the test solution. The weight loss measurements were carried out in a 100 ml capacity glass beaker placed in water thermostat. The specimens were then immediately immersed in the test solution without or with desired concentration of the investigated plant extract. Triplicate specimens were exposed for each condition and the mean weight losses were reported in order to verify reproducibility of the experiments. The inhibition efficiency (IE) and the degree of surface coverage (θ) of the investigated extract on corrosion of copper were calculated as follows:

$$\%IE = \theta \times 100 = [1 - (W/W^0)] \times 100 \quad (1)$$

Potentiodynamic polarization tests

Electrochemical experiments were performed in a conventional three-electrode electrochemical cell at 25°C with a platinum counter electrode and saturated calomel (SCE) as reference electrode. The working electrode was in the form of disc cut from the copper under investigation, first was immersed into the test solution for 30 min to establish a steady state open circuit potential. The potentiodynamic current-potential curves were recorded by changing the electrode potential automatically from -250 mV to +250 mV with scanning rate of 1mV s⁻¹ using Gamry framework instruments (version 3.20). Corrosion current densities (j_{corr}) and corrosion potential (E_{corr}), where evaluated from intersection of the linear anodic and cathodic branches of Tafel plots and all of them will calculated in absence and

presence of different concentrations of extract. Experiments were always repeated at least three times. Degree of surface coverage (θ) is calculated using the following equation:

$$\theta = (j_{\text{corr}} - j'_{\text{corr}}) / j_{\text{corr}} \quad (2)$$

and % IE were calculated as in Eq (3):

$$\% \text{ IE} = \theta \times 100 \quad (3)$$

where j_{corr} and j'_{corr} are the current densities in the absence and presence of extracts, respectively and θ is surface .

Electrochemical impedance spectroscopy (EIS) tests

Electrochemical impedance spectroscopy were performed at corrosion potentials, E_{corr} , over a frequency range of 10^{-5} Hz to 0.5 Hz with a signal amplitude perturbation of 10 mV. Data were presented as Nyquist and Bode plots. Experiments were always repeated at least three times. Degree of surface coverage (θ) and % IE were calculated using the following equations:

$$\theta = [(1/R'_{\text{ct}}) - (1/R_{\text{ct}})] / (1/R'_{\text{ct}}) \quad (4)$$

$$\% \text{ IE} = \theta \times 100 \quad (5)$$

where R'_{ct} and R_{ct} are the charge transfer resistance in the presence and absence of extract, respectively .

Electrochemical frequency modulation (EFM) tests

EFM experiments were performed with applying potential perturbation signal with amplitude 10 mV with two sine waves of 2 and 5 Hz. The choice for the frequencies of 2 and 5 Hz was based on three arguments [13-15]. The larger peaks were used to calculate the corrosion current density (i_{corr}), the Tafel slopes (β_a and β_c) and the causality factors CF-2 and CF-3 [16]

All electrochemical experiments were carried out using Gamry PCI300/4 Potentiostat/ Galvanostat/Zra analyzer, DC105 corrosion software, EIS300 electrochemical impedance spectroscopy software, EFM140 electrochemical frequency modulation software and Echem Analyst 5.21 for results plotting, graphing, data fitting and calculating.

Scanning electron microscopy (SEM) tests

The electron surface of copper was examined by Scanning Electron Microscope- type JOEL 840, Japan before and after immersion in 1 M HNO_3 test solution in the absence and presence of the optimum concentrations of the investigated extract at 25°C, for 2 days immersion time. The specimens were washed gently with bidistilled water, then dried carefully and examined without any further treatments.

Results and Discussion

Chemical methods (Weight loss method)

Weight-loss of copper was determined, at various time intervals, in the absence and presence of different concentrations of the extract. The obtained weight-loss time curves are represented in Figure 1 for senesio extract.

The inhibition efficiency of corrosion was found to be dependent on the extract concentration. The curves obtained in the presence of extract fall significantly below that of free acid. In all cases, the increase in the extract concentration was accompanied by a decrease in weight-loss and an increase in the percentage inhibition. These results lead to the conclusion that senesio extract under investigation is fairly efficient as extract for copper dissolution in nitric acid solution. Also, the degree of surface coverage (θ) by the extract, calculated from Eq. (1), would increase by increasing the extract concentrations.

Effect of Temperature

The effect of temperature on the corrosion rate of copper in 1M HNO_3 and in presence of different extract concentrations was studied in the temperature range of 298–313K using weight loss measurements. As the temperature increases, the rate of corrosion increases and the inhibition efficiency of the additives increase as shown in Table 3 for senesio extract. The adsorption

behavior of extract on copper surface occurs through chemical adsorption.

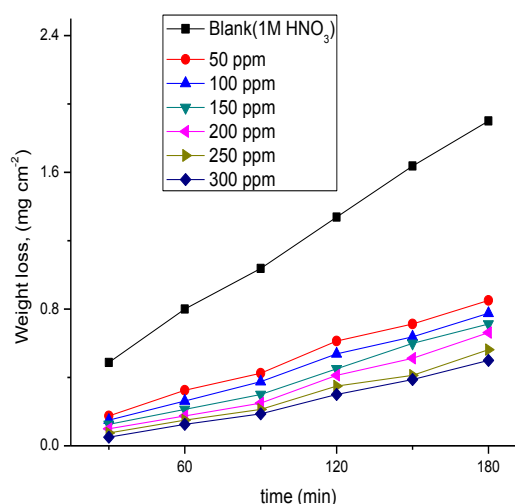


Figure 1. Weight loss-time curves for the corrosion of copper in 1 M HNO_3 in the absence and presence of different concentrations of senesio extract at 25°C

Adsorption isotherms

One of the most convenient ways of expressing adsorption quantitatively is by deriving the adsorption isotherm that characterizes the metal/extract/ environment system. Various adsorption isotherms were applied to fit θ values, but the best fit was found to obey Langmuir adsorption isotherm which are represented in Figure 2 for senesio extract, Langmuir adsorption isotherm may be expressed by:

$$C / \theta = 1 / K_{\text{ads}} + C \quad (6)$$

Where C is the concentration (m\l) of the extract in the bulk electrolyte, θ is the degree of surface coverage, K_{ads} is the adsorption equilibrium constant. A plot of θ versus C/θ should give straight lines. The experimental data gave good curves fitting for the applied adsorption isotherm as the correlation coefficients (R^2) were in the range (0.9808).

The values obtained are given in Table 4. The extent of inhibition is directly related to the performance of adsorption layer which is sensitive function of a molecular structure. The equilibrium constant of adsorption K_{ads} obtained from the intercepts of Langmuir adsorption isotherm is related to the free energy of adsorption $\Delta G_{\text{ads}}^\circ$ as follows

$$K = 1 / 55.5 \exp (-\Delta G_{\text{ads}}^\circ / RT) \quad (7)$$

Where, The value 55.5 is the concentration of water on the metal surface in mol/ L. Plot of $(\Delta G_{\text{ads}}^\circ)$ versus T gave the heat of adsorption ($\Delta H_{\text{ads}}^\circ$) and the entropy ($\Delta S_{\text{ads}}^\circ$) (Figure 5) according to the thermodynamic basic equation (8):

$$\Delta G_{\text{ads}} = \Delta H_{\text{ads}}^\circ - T \Delta S_{\text{ads}}^\circ \quad (8)$$

Table 5 clearly shows a good dependence of ΔG_{ads} on T , indicating the good correlation among thermodynamic parameters. The negative value of ΔG_{ads} reflects that the adsorption of studied extracts on copper surface from 1M HNO_3 solution is spontaneous process and stability of the adsorbed layer on copper surface.

Generally, values of ΔG_{ads} around -20 kJ mol^{-1} or lower are consistent with the electrostatic interaction between the charged molecules and the charged metal (physical adsorption); those around -40 kJ mol^{-1} or higher involves formation of coordinate bond (chemisorption) [17].

From the obtained values of $\Delta G_{\text{ads}}^\circ$ it was found the existence of comprehensive physical and chemical adsorption.

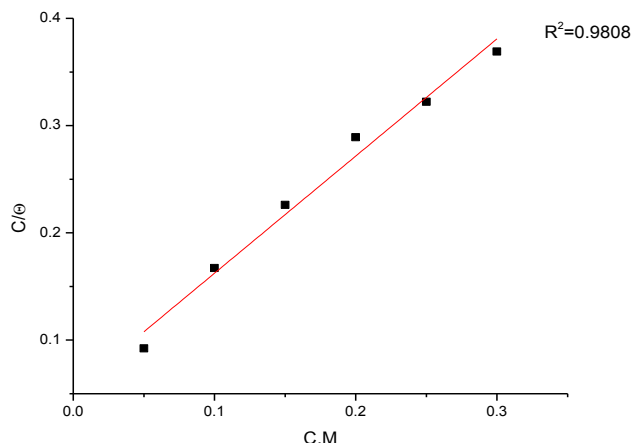


Fig 2. Langmuir adsorption isotherm plotted as C/θ vs. C of senesio extract for corrosion of copper in 1M HNO₃ solution from weight loss method at 298K

Plot of (ΔG°_{ads}) versus T Figure 3 gave the heat of adsorption (ΔH°_{ads}) and the standard entropy (ΔS°_{ads}) according to the thermodynamic basic equation 6:

$$\Delta G^{\circ}_{ads} = \Delta H^{\circ}_{ads} - T \Delta S^{\circ}_{ads} \tag{9}$$

Table 5 clearly shows a good dependence of ΔG°_{ads} on T, indicating the good correlation among thermodynamic parameters. The negative value of ΔG°_{ads} ensures the spontaneity of the adsorption process and stability of the adsorbed layer on copper surface. Generally, values of ΔG°_{ads} around -20 kJ mol^{-1} or lower are consistent with the electrostatic interaction between the charged molecules and the charged metal (physical adsorption). The calculated ΔG°_{ads} values are closer to -20 kJ mol^{-1} indicating that the adsorption mechanism of the extract on copper in 1 M HNO₃ solutions was typical of physical adsorption. The values of thermodynamic parameter for the adsorption of extract Table 5 can provide valuable information about the mechanism of corrosion inhibition. While an endothermic adsorption process ($\Delta H^{\circ}_{ads} > 0$) is attributed unequivocally to an exothermic adsorption process ($\Delta H^{\circ}_{ads} < 0$) may involve either exothermic adsorption or endothermic adsorption or mixture of both processes. In the presented case, the calculated values of ΔH°_{ads} for the adsorption of extract in 1 M HNO₃ indicating that chenopodium extract may be physically adsorbed. The ΔS°_{ads} values in the presence of extract in 1 M HNO₃ are positive. This indicates that an increase in disorder takes places on going from reactants to the metal-adsorbed reaction complex [18].

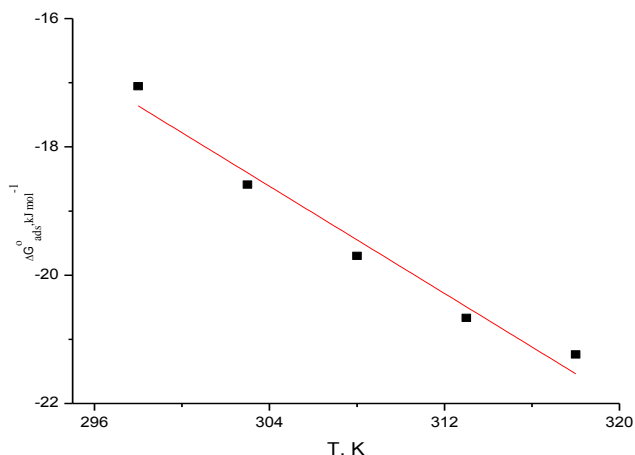


Figure 3. Variation of ΔG°_{ads} versus T for the adsorption of extract on copper surface in 1 M HNO₃ at different temperatures

Kinetic –Thermodynamic Corrosion Parameters

The activation parameters for the corrosion process were calculated from Arrhenius-type plot according to eq. (10):

$$k_{corr} = A \exp (E_a^*/RT) \tag{10}$$

Where E_a^* is the apparent activation corrosion energy, R is the universal gas constant, T is the absolute temperature and A is the Arrhenius pre-exponential constant. Values of apparent activation energy of corrosion for copper in 1 M HNO₃ shown in Table 6, without and with various concentrations of senesio extract determined from the slope of $\log (k_{corr})$ versus $1/T$ plots are shown in Figure 4. Inspection of the data shows that the activation energy is lower in the presence of extract than in its absence. This was attributed to slow rate of extract adsorption with a resultant closer approach to equilibrium during the experiments at higher temperatures according to Hoar and Holliday [19]. But, Riggs and Hurd [20] explained that the decrease in the activation energy of corrosion at higher levels of inhibition arises from a shift of the net corrosion reaction from the uncovered part of the metal surface to the covered one. Schmid and Huang [21] found that organic molecules inhibit both the anodic and cathodic partial reactions on the electrode surface and a parallel reaction takes place on the covered area, but the reaction rate on the covered area is substantially less than on the uncovered area similar to the present study. The alternative formulation of transition state equation is shown in Eq. (11):

$$k_{corr} = (RT/h) \exp (\Delta S^*/R) \exp (-\Delta H^*/RT) \tag{11}$$

Where k_{corr} is the rate of metal dissolution, h is Planck’s constant, N is Avogadro’s number, ΔS^* is the entropy of activation and ΔH^* is the enthalpy of activation.

Figure 5 shows a plot of $\log k/T$ against $(1/T)$ in 1 M HNO₃. Straight lines are obtained with aslopes equal to $(\Delta H^*/2.303R)$ and intercepts are $[\log (R/h) + \Delta S^*/2.303R]$ are calculated Table 6.

The increase in E_a^* with increase extract concentration Table 6 is typical of physical adsorption. The positive signs of the enthalpies (ΔH^*) reflect the endothermic nature of the copper dissolution process. Value of entropies (ΔS^*) imply that the activated complex at the rate determining step represents an association rather than a dissociation step, meaning that a decrease in disordering takes place on going from reactants to the activated complex [22,23].

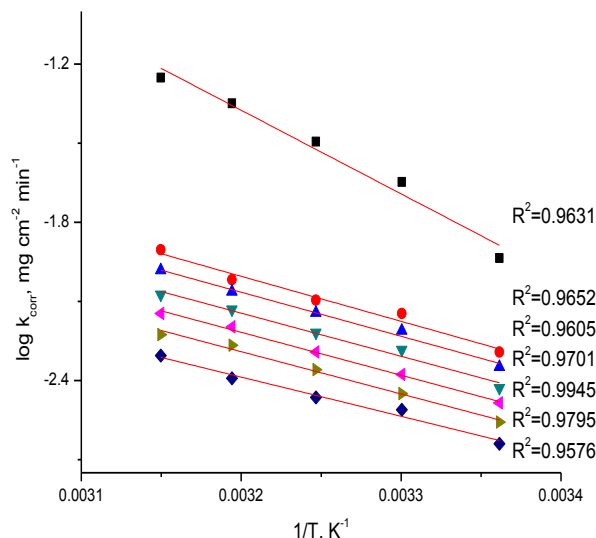


Figure 4. Arrhenius plots for copper corrosion rates (k_{corr}) after 120 minute of immersion in 1 M HNO₃ in the absence and presence of various concentrations of senesio extract

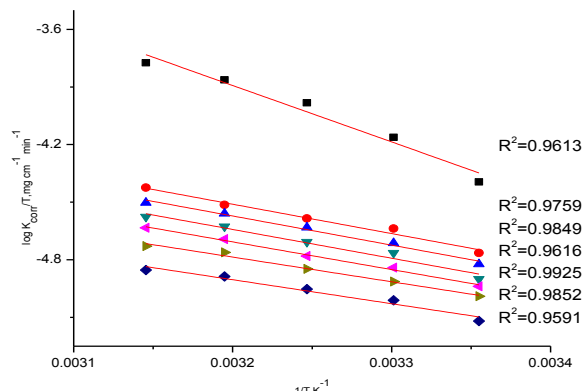


Figure 5. Transition-state for copper corrosion rates $\log(k_{\text{corr}}/T)$ vs $1/T$ in 1 M HNO_3 in the absence and presence of various concentrations of senesio extract

Potentiodynamic polarization measurements

Figures 6 show typical polarization curves for copper in 1 M HNO_3 media. The two distinct regions that appeared were the active dissolution region (apparent Tafel region), and the limiting current region. In the extract-free solution, the anodic polarization curve of copper showed a monotonic increase of current with potential until the current reached the maximum value. After this maximum current density value, the current density declined rapidly with potential increase, forming an anodic current peak that was related to $\text{Cu}(\text{NO}_3)_2$ film formation. In the presence of extract, both the cathodic and anodic current densities were greatly decreased over a wide potential range.

Various corrosion parameters such as corrosion potential (E_{corr}), anodic and cathodic Tafel slopes (β_a , β_c), the corrosion current density (j_{corr}), the degree of surface coverage (θ) and the inhibition efficiency (%IE) are given in Table 7. It can be seen from the experimental results that in all cases, addition of extract induced a significant decrease in cathode and anodic currents. The values of E_{corr} were affected and slightly changed by the addition of extract. This indicates that senesio extract acts as mixed-type extract. The slopes of anodic and cathodic Tafel lines (β_a and β_c), were slightly changed (Tafel lines are parallel), on increasing the concentration of senesio extract which indicates that there is no change of the mechanism of inhibition in the presence and absence of extract. The orders of inhibition efficiency of extract at different concentrations as given by polarization measurements are listed in Table 7. The results are in good agreement with those obtained from weight-loss measurements.

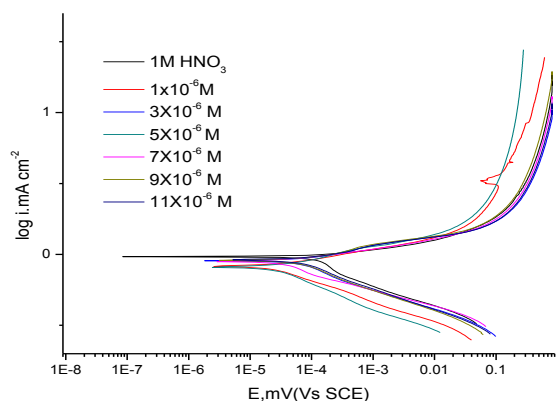


Figure 7. Potentiodynamic polarization curves for the dissolution of copper in 1M HNO_3 in absence and presence of different concentrations of senesio extract at 25°C

Electrochemical impedance spectroscopy (EIS) tests

well-established and it is powerful technique for studying the corrosion. Surface properties, electrode kinetics and mechanistic information can be obtained from impedance diagrams [24-28]. Figure 8 shows the Nyquist (a) and Bode (b) plots obtained at open-circuit potential both in the absence and presence of increasing concentrations of chenopodium extract at 25°C. The increase in the size of the capacitive loop with the addition of lemon oil shows that a barrier gradually forms on the copper surface. The increase in the capacitive loop size (Figure 8a) enhances, at a fixed extract concentration, following the order. Bode plots (Figure 8b), shows that the total impedance increases with increasing extract concentration ($\log Z$ vs. $\log f$). But ($\log f$ vs. phase), also Bode plot shows the continuous increase in the phase angle shift, obviously correlating with the increase of extract adsorbed on copper surface. The Nyquist plots do not yield perfect semicircles as expected from the theory of EIS. The deviation from ideal semicircle was generally attributed to the frequency dispersion [29] as well as to the inhomogeneities of the surface.

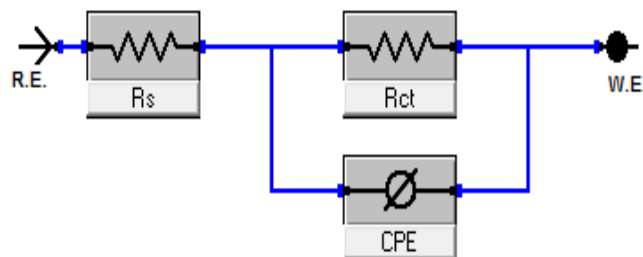


Figure 9. Equivalent circuit model used to fit experimental EIS

EIS spectra of the investigated compound were analyzed using the equivalent circuit, Figure 9, which represents a single charge transfer reaction and fits well with our experimental results. The constant phase element, CPE, is introduced in the circuit instead of a pure double layer capacitor to give a more accurate fit [30]. The double layer capacitance, C_{dl} , for a circuit including a CPE parameter (Y_0 and n) were calculated from eq.12 [31]:

$$C_{\text{dl}} = Y_0 (\omega_{\text{max}})^{n-1} \quad (12)$$

where Y_0 is the magnitude of the CPE, $\omega_{\text{max}} = 2\pi f_{\text{max}}$, f_{max} is the frequency at which the imaginary component of the impedance is maximal and the factor n is an adjustable parameter that usually lies between 0.50 and 1.0. After analyzing the shape of the Nyquist plots, it is concluded that the curves approximated by a single capacitive semicircles, showing that the corrosion process was mainly charged-transfer controlled [32,33]. The general shape of the curves is very similar for all samples (in presence or absence of extract at different immersion times) indicating that no change in the corrosion mechanism [34]. From the impedance data Table 8, we concluded that the value of R_{ct} increases with increasing the concentration of the extract and this indicates an increase in % IE_{EIS} , which in concord with the EFM results obtained. In fact the presence of extracts enhances the value of R_{ct} in acidic solution. Values of double layer capacitance are also brought down to the maximum extent in the presence of extract and the decrease in the values of CPE follows the order similar to that obtained for i_{corr} in this study. The decrease in CPE/C_{dl} results from a decrease in local dielectric constant and/or an increase in the thickness of the double layer, suggesting that organic derivatives inhibit the copper corrosion by adsorption at metal/acid [35, 36]. The inhibition efficiency was calculated from the charge transfer resistance data from eq.13 [37]:

$$\% IE_{EIS} = [1 - (R_{ct}^0 / R_{ct})] \times 100 \quad (13)$$

Where R_{ct}^0 and R_{ct} are the charge-transfer resistances without and with extract, respectively

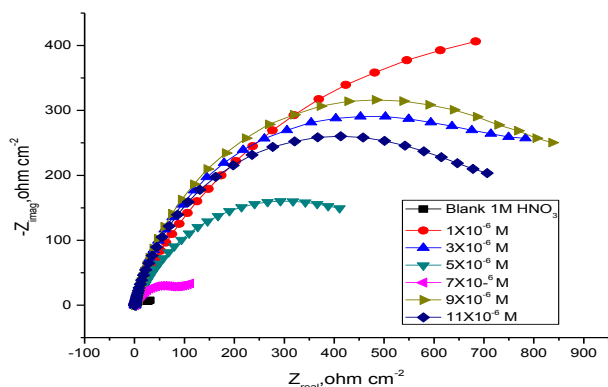


Figure 8a. The Nyquist plots for corrosion of copper in 1M HNO₃ in absence and presence of different concentrations of senesio extract at 25°C

senesio extract at a given concentration to the acidic solution decreases the corrosion current density, indicating that this compound inhibits the corrosion of copper in 1 M HNO₃ through adsorption. The causality factors obtained under different experimental conditions are approximately equal to the theoretical values (2 and 3) indicating that the measured data are verified and of good quality. The inhibition efficiencies %IE_{EFM} increase by increasing the extract concentrations and was calculated as from Eq. (14):

$$\% IE_{EFM} = [1 - (j_{corr} / j_{corr}^0)] \times 100 \quad (14)$$

Where j_{corr} and j_{corr}^0 are corrosion current densities in the absence and presence of senesio extract

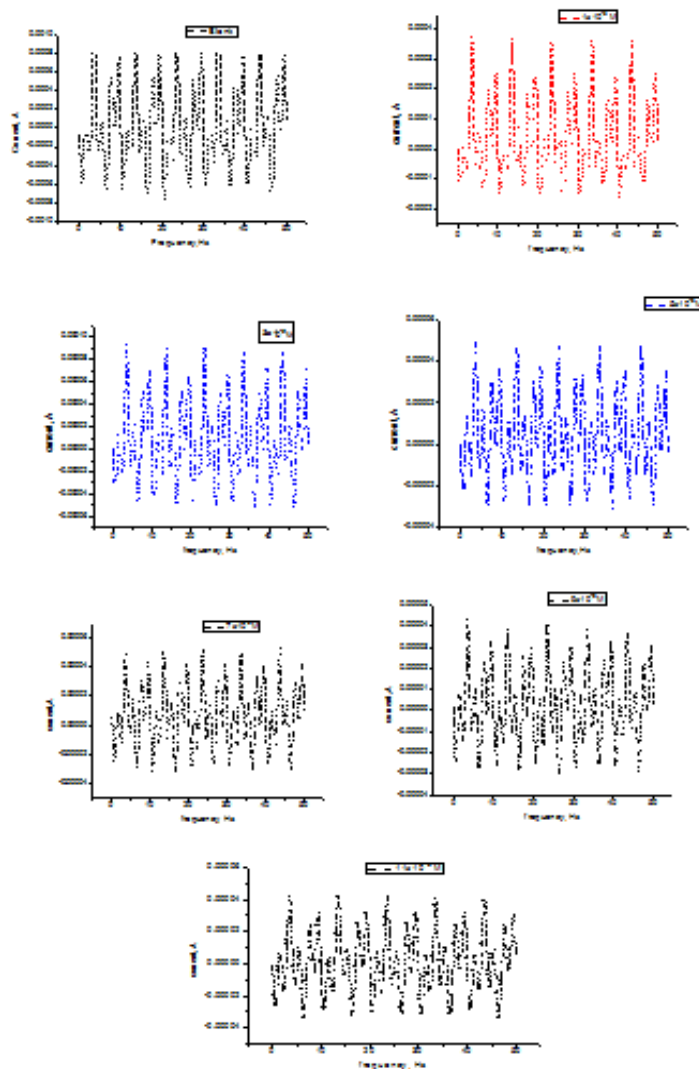


Figure 10. EFM spectra for copper in 1M HNO₃ in absence and presence of different concentrations of senesio extract at 25°C

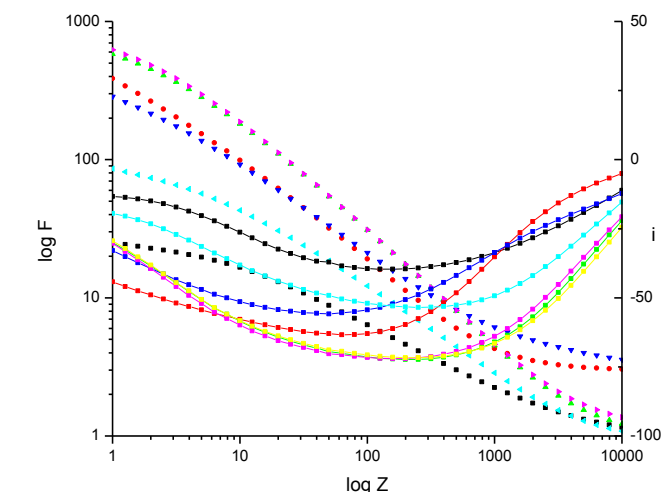


Figure 9b. The Bode plots for the corrosion of copper in 1M HNO₃ in absence and presence of different concentrations of senesio extract at 25°C

Electrochemical frequency modulation (EFM) tests

EFM is a nondestructive corrosion measurement technique that can directly and quickly determine the corrosion current values without prior knowledge of Tafel slopes, and with only a small polarizing signal. These advantages of EFM technique make it an ideal candidate for online corrosion monitoring [38]. The great strength of the EFM is the causality factors which serve as an internal check on the validity of EFM measurement. The causality factors CF-2 and CF-3 are calculated from the frequency spectrum of the current responses.

Figure 10 shows the EFM Intermodulation spectra (current vs frequency) of copper in HNO₃ solution containing different concentrations of senesio extract. The experimental EFM data were treated using two different models: complete diffusion control of the cathodic reaction and the “activation” model. For the latter, a set of three non-linear equations had been solved, assuming that the corrosion potential does not change due to the polarization of the working electrode [39]. The larger peaks were used to calculate the corrosion current density (j_{corr}), the Tafel slopes (β_c and β_a) and the causality factors (CF-2 and CF-3). These electrochemical parameters were listed in Table 9. The data presented in Table 9 obviously show that, the addition of

SEM examination

In order to verify if the senesio extract molecules are in fact adsorbed on copper surface, SEM experiments were carried out. The SEM micrographs for copper surface alone and after 48 h immersion in 1 M HNO₃ without and with the addition of 11x10⁻⁶ M of senesio extract are shown in Figures (11a-c). As expected, Figure 11a shows metallic surface is clear, while in the absence of senesio extract, the copper surface is damaged by HNO₃ corrosion (Figure 11b). In contrast, in presence of the investigated compound (Figures (11c)); the metallic surface seems to be almost no affected by corrosion. The formation of a thin film of senesio extract observed in SEM micrograph protects the surface against corrosion.

Table 1. chemical composition of the copper in weight %

Element	Sn	Ag	Fe	Bi	Pb	As	Cu
Weight %	0.001	0.001	0.01	0.0005	0.002	0.0002	The rest

Table 2. Values of inhibition efficiencies (%IE) and surface coverage (θ) of extract for the corrosion of copper in 1 M HNO₃ from weight-loss measurements at different concentrations and at 25°C

[inh]x10 ⁶ , M	θ	%IE
1	0.542	54.2
3	0.598	60.0
5	0.663	66.3
7	0.691	69.1
9	0.738	73.8
11	0.775	77.5

Table 3. Values of inhibition efficiencies %IE and corrosion rate (C.R) of senesio extract for the corrosion of copper in 1M HNO₃ from weight-loss measurements at different concentrations at temperature range of 298-313 K

[Inh]x10 ⁶ , M	298		303K		308K		313K		318K	
	C.R	%IE								
1	5.10	54.2	6.97	69.1	8.02	75.0	9.58	77.7	10.0	79.7
3	4.47	60.0	6.14	72.8	7.18	77.5	8.64	80.0	9.58	82.0
5	3.75	66.3	5.20	77.0	6.04	81.1	7.39	82.7	8.43	84.2
7	3.43	69.1	4.37	80.6	5.14	84.0	6.35	85.1	7.39	86.1
9	2.50	73.8	3.95	82.5	4.37	86.3	5.41	87.3	5.93	88.8
11	2.08	77.5	3.12	86.1	3.43	89.2	4.06	90.5	4.45	91.7

Table 4. Adsorption parameters for senesio extract in 1 M HNO₃ obtained from Langmuir adsorption isotherm at different temperatures

Temperature, °C	K _{ads} , M ⁻¹	slope
25	16.7	1.052
30	36.4	1.086
35	45.1	1.059
40	50.6	1.054
45	55.4	1.045

Table 5. Thermodynamic parameters for the adsorption of senesio extract on copper surface in 1 M HNO₃ at different temperatures

Temperature, °C	- ΔG°_{ads} , kJ mol ⁻¹	ΔH°_{ads} , kJ mol ⁻¹	ΔS°_{ads} , J mol ⁻¹
25	16.9	44.8	207.3
30	19.1		211.2
35	20.0		210.6
40	20.6		209.3
45	21.2		207.8

Table 6. Activation parameters for copper corrosion in the absence and presence of various concentrations of senesio extract in 1M HNO₃

[Inh]x10 ⁶ M	E _a [*] , kJ mol ⁻¹	ΔH° , kJ mol ⁻¹	- ΔS° , J mol ⁻¹ K ⁻¹
0	60.69	56.23	196.99
1	32.66	29.26	190.18
3	31.98	29.04	192.03
5	31.31	28.69	194.49
7	31.13	27.59	199.27
9	30.69	24.63	210.25
11	28.50	23.93	214.75

Table 7. Corrosion potential (E_{corr}), corrosion current density (j_{corr}), Tafel slopes (β_a , β_c), degree of surface coverage(θ) and inhibition efficiency (%IE) of copper in 1M HNO₃ at 25°C for senesio extract

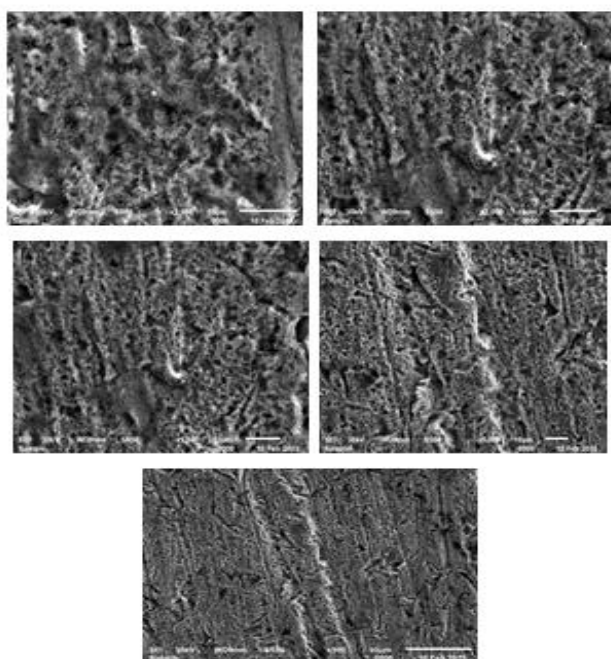
[Inh]x10 ⁶ M	E _{corr} , mV vs SCE	j _{corr} , μ A cm ⁻²	β_a , mV dec ⁻¹	β_c , mV dec ⁻¹	C.R mpy	θ	% IE
Blank	16	512.0	318	222	252.6	-----	-----
1	45	66.40	72	207	32.75	0.870	87.0
3	39	65.80	71	189	32.47	0.871	87.1
5	43	64.70	75	198	31.92	0.874	87.4
7	49	37.60	59	203	18.56	0.926	92.6
9	89	33.50	100	228	16.53	0.935	93.5
11	83	28.00	71	217	13.83	0.945	94.5

Table 8. Electrochemical kinetic parameters obtained by by EIS technique for in 1 M HNO₃ without and with various concentrations of senesio extract at 25°C

Extract	[inh]x10 ⁶ M	R _p , Ω cm ²	C _{dl} x10 ⁻⁴ , μFcm ⁻²	Θ	% IE
Blank	0	28.6	6.05	----	-----
senesio	1	104.1	3.40	0.725	72.5
	3	523.2	3.51	0.945	94.5
	5	688.3	1.13	0.958	95.8
	7	800.7	8.65	0.964	96.4
	9	835.7	1.02	0.966	96.6
	11	934.3	3.39	0.97	97.0

Table 9. Electrochemical kinetic parameters obtained by EFM technique for copper in the absence and presence of various concentrations of senesio extract in 1M HNO₃ at 25°C

Inh.	Conc,x10 ⁶ M	j _{corr} μAcm ⁻²	β _a mVdec ⁻¹	β _c mVdec ⁻¹	CF-2	CF-3	C.R Mpy	Θ	% IE
Blank	0	523.7	64	92	2.325	3.897	258.5	----	-----
Senesio extract	1	193	64	169	1.933	2.899	95.22	0.631	63.1
	3	43.99	67	102	1.865	2.614	21.71	0.916	91.6
	5	33.34	90	159	1.783	2.831	16.45	0.936	93.6
	7	31.9	48	128	1.834	2.490	15.74	0.939	93.9
	9	30.62	34	151	2.048	2.737	15.11	0.941	94.1
	11	29.55	89	129	1.967	2.919	14.58	0.944	94.4

**Figure 11. SEM micrographs of copper surface (a) before of immersion in 1 M HNO₃, (b) after 48 h of immersion in 1 M HNO₃, (c) after 48 h of immersion in 1 M HNO₃+ 11x10⁻⁶ M of senesio extract at 25°C****Mechanism of Corrosion Inhibition**

The inhibition mechanism involves the adsorption of the extract components on the copper surface immersed in aqueous HNO₃ solution. Four types of adsorption [40] may take place involving organic molecules at the metal–solution interface: 1) Electrostatic attraction between the charged molecules and the charged metal; 2) Interaction of unshared electron pairs in the molecule with the metal; 3) Interaction of π-electrons with the metal; 4) Combination of all the above. From the observations drawn from the different methods, corrosion inhibition of copper in 1M HNO₃ solutions by senesio extract as indicated from weight loss, potentiodynamic polarization and EIS techniques

were found to depend on the concentration and the temperature of the medium.

Conclusions

- From the results of the study the following may be concluded:
- 1-Senesio extract is good corrosion inhibitors for copper in 1 M HNO₃ solution.
 - 2- Reasonably good agreement was observed between the values obtained by the weight loss and electrochemical measurements.
 - 3-Results obtained from potentiodynamic polarization indicated that senesio extract is mixed-type inhibitor.
 - 4- Percentage inhibition efficiency of senesio extract was temperature dependent and its addition led to a decrease of the activation corrosion energy in all the studied acid media.
 - 5- The thermodynamic parameters revealed that the inhibition of corrosion by senesio extract is due to the formation of a physical adsorbed film on the metal surface.
 - 6- The adsorption of senesio extract onto copper surface follows the Langmuir adsorption isotherm model.
 - 7- The negative values of the free energy of adsorption and the positive values of heat of adsorption are indicating that the process was spontaneous and endothermic.

References

- [1] A.Igual Muñoz, J. García Antón, J.L. Guñón, V. Pérez Herranz, Comparison of inorganic extracts of copper, nickel and copper–nickels in aqueous lithium bromide solution, *Electrochimica Acta* 50(4) (2004)957-966
- [2] M.S. Al-Otaibi, A.M. Al-Mayouf, M. Khan, A.A. Mousa, S.A. Al-Mazroa, H.Z. Alkathlan, Corrosion inhibitory action of some plant extracts on the corrosion of mild steel in acidic media, *Arabian J.Chem.*, 7(3)(2014)340-346
- [3] E.E. Oguzie, Studies on the inhibitive effect of *Occimum viridis* extract on the acid corrosion of mild steel, *Mater. Chem. Phys.* 99 (2–3) (2006) 441-446
- [4] A.Y. El-Etre, Inhibition of aluminum corrosion using *Opuntia* extract, *Corros. Sci.* 45 (2003) 2485-2495
- [5] O.Mojisola Nkiko, Janet T. Bamgbose, Corrosion Inhibitive Effect of *Ocimum Gratissimum* Extract on Zinc – Aluminium Alloy in Hydrochloric Acid, *Port. Electrochim Acta* 29(2011) 419-427

- [6] M. Kliskic, J. Radosevic, S. Gudic, V. Katalinik, Aqueous extract of *Rosmarinus officinalis* L. as inhibitor of Al–Mg alloy corrosion in chloride solution, *J. Appl. Electrochem.* 30 (2000) 823-830
- [7] Nnabuk Okon Eddy, Benedict I. Ita, Simon N. Dodo, Elaoyi D. Paula, Inhibitive and adsorption properties of ethanol extract of *Hibiscus sabdariffa* calyx for the corrosion of mild steel in 0.1 M HCl, *Green Corrs.Lett.Rev.*, 5(2012)45-53
- [8] S.A. Umoren, U.M. Eduok, A.U. Israel, I.B. Obot, M.M. Solomon, Coconut coir dust extract: a novel eco-friendly corrosion inhibitor for Al in HCl solutions, *Green Corrs.Lett.Rev.*, 5(2012) 303-312
- [9] E.I. Ating, S.A. Umoren, I.I. Udousoro, E.E. Ebenso, A.P. Udoh, Leaves extract of *Ananas sativum* as green corrosion inhibitor for aluminium in hydrochloric acid solutions, *Green Corrs.Lett.Rev.*, 3(2010)61-68
- [10] K. Sanjay Sharma, Ackmez Mudhoo, Gargi Jain, Jyoti Sharma, Corrosion inhibition and adsorption properties of *Azadirachta indica* mature leaves extract as green inhibitor for mild steel in HNO₃, *Green Corrs.Lett.Rev.*, 3(2010) 7-15
- [11] Z.V.P. Murthy, K. Vijayaragavan, Mild steel corrosion inhibition by acid extract of leaves of *Hibiscus sabdariffa* as a green corrosion inhibitor and sorption behavior, *Green Corrs.Lett.Rev.*, 7(2014) 209-219
- [12] Nnabuk O. Eddy*, Stevens A. Odoemelamb & Ibiam N. Amab, Ethanol extract of *Ocimum gratissimum* as a green corrosion inhibitor for the corrosion of mild steel in H₂SO₄, *Green Corrs.Lett.Rev.*, 3(2010) 165-172
- [13] K. F. Khaled, *Mater. Chem. Phys.*, Application of electrochemical frequency modulation for monitoring corrosion and corrosion inhibition of iron by some indole derivatives in molar hydrochloric acid, *Mater. Chem. Phys.*, 112, (2008) 290-300.
- [14] K. F. Khaled, Evaluation of electrochemical frequency modulation as a new technique for monitoring corrosion and corrosion inhibition of carbon steel in perchloric acid using hydrazine carbodithioic acid derivatives, *J. Appl. Electrochem.*, *J. Appl. Electrochem.*, 39, (2009), 429-438.
- [15] R. W. Bosch, J. Hubrecht, W. F. Bogaerts, B. C. Syrett, Electrochemical frequency modulation: a new electrochemical technique for online corrosion monitoring, *Corrosion.*, 57(1) (2001) 60-70 .
- [16] S. S. Abdel-Rehim, K. F. Khaled, N. S. Abd-Elshafi, Electrochemical frequency modulation as a new technique for monitoring corrosion inhibition of iron in acid media by new thiourea derivative, *Electrochim. Acta.*, 51(16) (2006) 3269-3277.
- [17] A. Yurt, G. Bereket, A. Kivrak, A. Balaban and B. Erk, Effect of Schiff bases containing pyridyl group as corrosion extracts for low carbon steel in 0.1 M HCl, *J Appl Electrochem*, 35(10) (2005) 1025-1032
- [18] G. Banerjee and S N. Malhotra, Contribution to adsorption of aromatic amines on mild steel surface from HCl solutions by impedance, *Corrosion.*, 48(1) (1992) 10-15.
- [19] T. P. Hour and R. D. Holliday, The inhibition by quinolines and thioureas of the acid dissolution of mild steel, *J Appl Chem.*3(11) (1953) 502-513.
- [20] L. O. Riggs (Jr) and T. J. Hurd, Temperature coefficient of corrosion inhibition, *Corrosion.* 23(8) (1967) 252-260.
- [21] G M Schmid & H J Huang, Spectro-electrochemical studies of the inhibition effect of 4, 7-diphenyl -1, 10-phenanthroline on the corrosion of 304 stainless steel, *Corros Sci.* 20(8-9), (1980), 1041-1057.
- [22] F Bentiss, M Lebrini & M Lagrenee, Thermodynamic characterization of metal dissolution and extract adsorption processes in mild steel/2,5-bis(n-thienyl)-1,3,4-thiadiazoles/hydrochloric acid system, *Corros Sci.*, 47(12), (2005) 2915-2931.
- [23] Marsh J, *Advanced Organic Chemistry*, 3rd edn (Wiley Eastern, New Delhi), 1988.
- [24] D.C. Silverman and J. E. Carrico, Electrochemical impedance technique—a practical tool for corrosion prediction, *Corrosion.* 44(5) (1988) 280-287. [25] W. J. Lorenz and F. Mansfeld, Determination of corrosion rates by electrochemical DC and AC methods, *Corros.Sci.*, 21(9-10), (1981) 647-672.
- [26] Macdonald D. D., Mckubre M. C., "Impedance measurements in Electrochemical systems," *Modern Aspects of Electrochemistry*, J.O'M. Bockris, B.E. Conway, R.E.White, Eds., Plenum Press, New York, New York, 1982, 14 61, .
- [27] F. Mansfeld; Recording and analysis of AC impedance data for corrosion studies, *Corrosion.*, 37(5) (1981) 301-307.
- [28] C. Gabrielli, "Identification of Electrochemical processes by Frequency Response Analysis," *Solartron Instrumentation Group*, 1980.
- [29] M. El Achouri, S. Kertit, H.M. Goultaya, B. Nciri, Y. Bensouda, L. Perez, M.R. Infante, K. Elkacemi, Corrosion inhibition of iron in 1 M HCl by some gemini surfactants in the series of alkanediyl- α,ω -bis-(dimethyl tetradecyl ammonium bromide, *Prog. Org. Coat.*, 43(4), (2001), 267-273.
- [30] Macdonald J.R., Johanson W.B., in: J.R. Macdonald (Ed.), *Theory in Impedance Spectroscopy*, John Wiley & Sons, New York, 1987.
- [31] S. F. Mertens, C. Xhoffer, B. C. Decooman, E. Temmerman, Short-Term Deterioration of Polymer-Coated 55% Al-Zn — Part 1: Behavior of Thin Polymer Films, *Corrosion.*, 53, (1997) 381-388.
- [32] G. Trabaneli, C. Montecelli, V. Grassi, A. Frignani, Electrochemical study on extracts of rebar corrosion in carbonated concrete, *J. Cem. Concr., Res.*, 35 (2005) 3
- [23] A. J. Trowsdate, B. Noble, S. J. Haris, I.S. R. Gibbins, G. E. Thomson, G. C. Wood, The influence of silicon carbide reinforcement on the pitting behaviour of aluminium, *Corros. Sci.*, 38(2) (1996) 177-191.
- [34] F. M. Reis, H.G. De Melo and I. Costa, EIS investigation on Al 5052 alloy surface preparation for self-assembling monolayer, *Electrochim. Acta.*, 51 (2006) 1780-1788.
- [35] M. Lagrenee, B. Mernari, M. Bouanis, M. Traisnel & F. Bentiss, Study of the mechanism and inhibiting efficiency of 3,5-bis(4-methylthiophenyl)-4H-1,2,4-triazole on mild steel corrosion in acidic media, *Corros. Sci.*, 44(3), (2002) 573-588.
- [36] E. McCafferty, N. Hackerman, Double layer capacitance of iron and corrosion inhibition with polymethylene diamines, *J. Electrochem. Soc.*, 119 (1972) 146-154.
- [37] H. Ma, S. Chen, L. Niu, S. Zhao, S. Li, D. Li, Inhibition of copper corrosion by several Schiff bases in aerated halide solutions, *J. Appl. Electrochem.*, 32(1) (2002) 65-72.
- [38] E. Kus, F. Mansfeld, An evaluation of the electrochemical frequency modulation (EFM) technique, *Corros. Sci.*, 48(4), (2006) 965-979.
- [39] G. A. Caigman, S. K. Metcalf, E. M. Holt, Thiophene substituted dihydropyridines, *J.Chem. Cryst.*, 30(6) (2000) 415-422.
- [40] D. P. Schweinsberg, G. A. Graeme, A.K. Nanayakkara and D. A. Steinert, The protective action of epoxy resins and curing agents-inhibitive effects on the aqueous acid corrosion of iron and steel," *Corros. Sci.*, 28(1), (1988) 33-42